3rd Turkish Conference on Earthquake Engineering and Seismology
October 14-16, 2015, Izmir/Turkey

SEISMIC DAMAGE ASSESSMENT USING SYNTHETIC GROUND MOTIONS: A CASE STUDY FOR ERZINCAN

S. Karimzadeh[1], A. Askan[2], M.A. Erberik[3] and A. Yakut[4]

[1] *Research Assistant, Civil Engineering Department, Middle East Technical University, Ankara*
[2] *Associate Professor, Civil Engineering Department, Middle East Technical University, Ankara*
[3] *Professor, Civil Engineering Department, Middle East Technical University, Ankara*
[4] *Professor, Civil Engineering Department, Middle East Technical University, Ankara*
Email: shaghayegh.karimzadehnaghshineh@metu.edu.tr

ABSTRACT:

Estimation of seismic losses is a fundamental step for risk mitigation decision-making in urban regions. As the study region, Erzincan, a city on the eastern part of Turkey is selected which is located in the conjunction of three active faults as right lateral North Anatolian Fault, left lateral North East Anatolian Fault and left lateral Ovacik fault. Erzincan city center is in a pull-apart basin underlain by soft sediments that has experienced devastating earthquakes such as the 27 December 1939 (Ms~8.0) and the 13 March 1992 (Mw=6.6) events, resulting in extensive amount of economic losses, physical damage, and large number of fatalities. This is due to not only the high seismicity of the area but also as a result of the seismic vulnerability of the constructed environment. Therefore, in this study, the seismic damage estimation of Erzincan is carried out considering both regional seismicity and local building information. For this purpose, first, ground motion records are selected from a set of scenario events generated with the stochastic finite fault methodology using regional seismicity parameters. Then, existing building stock are classified into specified groups that are represented with equivalent single-degree-of-freedom systems where the inelastic dynamic structural characteristics of the models are investigated. The response statistics of the structures are evaluated through non-linear time history analysis. Fragility Curves for the classified structural types are derived and discussed. Finally, the estimated damage is compared with the observed damage during the 1992 Erzincan earthquake. The results seem to have a reasonable match in between.

KEYWORDS : Fragility Analysis, Erzincan, Regional Seismicity, Stochastic Finite-fault Method, Local Buildings, Nonlinear Time History Analysis.

1. INTRODUCTION

Estimation of seismic risk and damage is crucial in seismically active countries such as Turkey. Identification of seismic risk in any area is performed in two steps. The first step is assessment of potential seismic hazard in that region of interest by performing seismic hazard analyses, while the second step is vulnerability analysis including derivation of fragility curves and building damage assessment. This study concentrates on seismic damage assessment based on simulated ground motions and local building data.

For estimation of earthquake damage and loss due to near field large events, it is important to consider the effect of the earthquake rupture process. In regions with sparse ground motion data, ground motion simulations provide alternative time histories accounting for the specific features of the fault and the kinematics of the rupture process.

In addition, local building data is of particular interest to physically model the building damage and consequent losses. Majority of the building stock in different parts of Turkey consists of low-rise and mid-rise reinforced concrete (RC) frame structures as well as unreinforced masonry buildings. However, most of these structures

have deficiencies and they are not designed according to seismic design codes to resist strong ground shaking. Therefore, it is critical to investigate the seismic risk of any region of interest by considering the regional building stock.

Until recently, majority of the past studies related to damage and loss estimation used generic information regarding either the building stock or ground motion records. However, there are few studies (e.g.: Ugurhan et al., 2011 and Sørensen et al., 2015) on development of seismic fragility curves by the means of both regional building characteristics and seismicity of the area of interest.

In this study, as the study region, Erzincan in the Eastern of Turkey, located in the close vicinity of the North Anatolian Fault Zone (NAFZ) is selected. It is aimed herein to assess the seismic damage of a specified region by using both local structural parameters as well as regional synthetic ground motion records of the corresponding study area. To validate the proposed methodology, the estimated damage is compared with the observed damage during the 1992 Erzincan earthquake. Finally, the potential seismic damage for a scenario event in the region with Mw=7 is presented.

2. STUDY REGION

North Anatolian Fault (NAFZ) is an active right-lateral strike-slip fault that lies in Northern Turkey and is one of the most active fault zones in the world. In the last century, NAFZ led to the most destructive events in Turkey such as the 1939 Erzincan (Ms~8.0) event in the eastern part (Figure 1) as well as the 1999 Kocaeli (Mw=7.4) and 1999 Düzce (Mw=7.2) earthquakes in the western part close to Istanbul.

Erzincan is one of the most hazardous cities in Eastern Turkey located in a tectonically complicated area, at the conjunction of three strike slip faults: the right lateral North Anatolian Fault, the left lateral North East Anatolian Fault, and the left lateral Ovacik fault. In addition to the 1939 event, Erzincan suffered from another destructive earthquake in 1992 (Mw=6.6) that led to significant structural damage as well as mortalities (Figure 1).

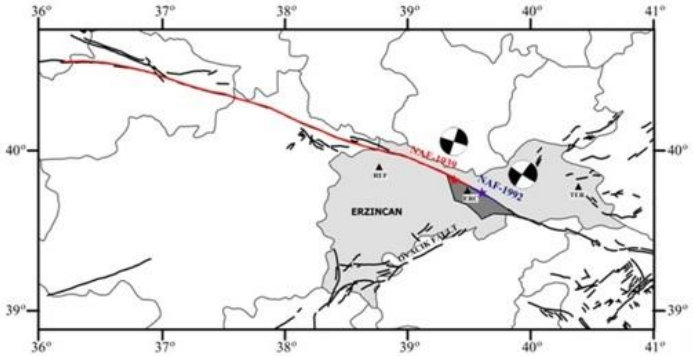

Figure 1. Seismotectonics in the Erzincan region with the fault systems and the epicenters of the 1939 and 1992 events

According to the General Statistic Agency in Turkey (TÜİK), majority of the buildings in Erzincan (79%) are residential. Thus, the focus of this study is damage estimation of only residential buildings.

3. GROUND MOTION SIMULATIONS

3.1. Methodology: Stochastic ground motion simulations

Estimation of reliable synthetic time histories is the fundamental target of all ground motion simulation techniques varying from deterministic to stochastic models. Methods to simulate ground motions can be divided into three main groups: deterministic, stochastic and hybrid simulations. Deterministic approaches require exactly defined seismic sources as well as highly-resolved velocity models to accomplish the numerical solution

of the wave equation for full wave propagation purposes (e.g.: Olsen et al. 1996). They are mostly practical for relatively lower frequencies. Stochastic techniques combine the deterministic far field S-wave spectrum with random phases (Boore, 1983). These methods have intrinsic limitations due to absence of full wave propagation effects, however they are used efficiently worldwide for numerous seismic regions in the form of either point-source or finite-fault modeling (e.g.: Motazedian and Atkinson, 2005; Ugurhan and Askan, 2010). Hybrid methods combine deterministic and stochastic approaches for the simulation of low and high frequency components, respectively (e.g.: Mai et al., 2010).
In this study, since there exist no high-resolution velocity models of shallow soil layers for Erzincan region, deterministic models are out of scope. A recent form of stochastic finite-fault modeling which was shown to provide realistic broadband frequencies for engineering purposes is used.

3.2. Simulations along Eastern segment of NAFZ

Erzincan is a city with relatively sparse ground motion networks. Therefore, in this section, it is aimed to perform ground motion simulations for scenario earthquakes of size Mw=5.0, 5.5, 6.0, 6.5, 7.0, and 7.5 as well as the 1992 event using stochastic finite fault methodology as implemented in the computer program EXSIM, (Motazedian and Atkinson, 2005) .
In the present study, the region of interest is defined as a rectangular box bounded by 39.45°-39.54° longitudes, 39.70°-39.78° latitudes. Then, to simulate horizontal components of full time series of ground motions, a total of 123 grid points are selected inside of this region.
The source, path and site parameters for the simulations are adopted from a previous study by Askan et al. (2013).
Figure2 illustrates the spatial distribution of the simulated peak ground acceleration (PGA) and peak ground velocity (PGV) within the city center for the 1992 Erzincan earthquake (Mw=6.6) as a sample. It is worth to mention that all of the generated earthquakes are baseline corrected and 4th order bandpass filtered at 0.25-25 Hz. The results of the predicted 1992 Erzincan earthquake yield that the city center experiences maximum PGA and PGV values of around 1g and 85 cm/sec, respectively. As stated previously, Erzincan city center is placed on a deep alluvial basin in the close vicinity of the fault plane. It was recorded that, in spite of the moderate size of 1992 Erzincan earthquake, the residential structures suffered from significant levels of damage during the earthquake. Thus, these higher amplitudes of anticipated seismic intensities are believed to explain the observed widespread fatalities.

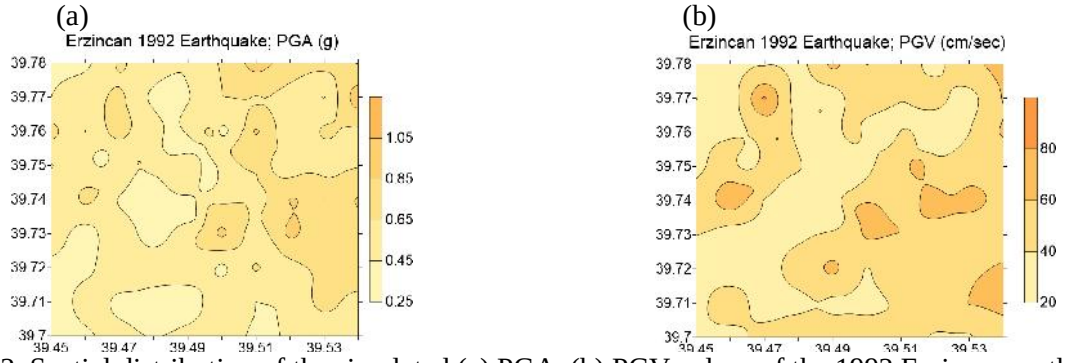

Figure 2. Spatial distribution of the simulated (a) PGA, (b) PGV values of the 1992 Erzincan earthquake

4. CLASSIFICATION OF THE REGIONAL BUILDING STOCK

Based on the results of a walk-down survey in the city center of Erzincan, all building stock is classified into 21 groups including 12 reinforced concrete and 9 masonry subclasses. Among these subclasses, reinforced concrete structures are considered as either frame type, shear wall type (actually tunnel form) or dual type (i.e. frame with

shear walls). Major structural parameters used in the classification of buildings are structural type, number of stories and level of compliance with the seismic design and construction principles. In classification of all subclasses, the first two letters in the abbreviated names account for the type of structural system, where 'RF' stands for RC frame buildings, 'RW' for RC tunnel-form, 'RH' for RC dual-type, and 'MU' for unreinforced masonry subclasses. The number in the next digit indicates the number of stories, where for masonry classes '1', '2', or '3' represents 1 story, 2 story, or 3 story, and for all three RC groups, '1' or '2' indicates whether the building is low-rise (number of the story is between 1 and 3) or mid-rise (number of stories is between 4 and 8), respectively. The letter in the last digit 'A', 'B', or 'C' denotes the high, moderate, and low level of compliance with seismic design codes and construction principles. For example, RF2A represents earthquake-resistant mid-rise RC frame buildings whereas MU2C represents deficient (with many violations regarding earthquake resistant design and construction principles) 2 story masonry buildings.
In this study, to derive fragility curves, multi degree of freedom (MDOF) systems are idealized as equivalent single degree of freedom (ESDOF) systems by specifying 3 basic structural parameters; period (T), strength ratio (η), and ductility factor (μ). These parameters are obtained from idealization of the capacity curve of each building. The mean and standard deviation of the corresponding ESDOF parameters are calculated for each subclass.

5. NONLINEAR TIME HISTORY ANALYSIS

For the statistical evaluation of engineering demand parameters, nonlinear time history analysis (NLTHA), which simulates the actual structural behavior under severe earthquake shaking is performed. To conduct NLTHA, OpenSees program developed by the University of California-Berkeley is used in this study, (http://opensees.berkeley.edu). ESDOF displacement is used as the seismic demand parameter for the considered building types.

5.1. Hysteresis model used

One of the most important tasks in NLTHA of the ESDOF systems is the use of a proper hysteresis model capable of estimating the inelastic behavior of the real structural systems under earthquake excitations in a reasonably accurate way. There exist many hysteresis models in the literature that take into account the possible deterioration modes such as reloading and unloading stiffness degrading, capping and cyclic strength degrading and pinching (e.g. :Park et al. 1987, Sucuoğlu and Erberik 2004).Structures are generally subjected to significant strength and stiffness deterioration while they approach collapse. As a matter of fact, new and well-constructed structures are expected to exhibit almost none or slight degradation. However, most existing buildings in Turkey include many structural deficiencies which result in rapid degradation of stiffness and strength along with decreased energy dissipation capacity. Therefore, the most accurate hysteresis models are the ones including strength and stiffness deterioration features that are critical for demand predictions during major earthquakes. In this study, to assess the effect of deterioration characteristics of structural systems on the final fragility curves, among different hysteresis models, the one proposed by Ibarra et al. (2005), named as Modified Ibarra – Medina-Krawinker Deterioration Model, is applied. Ibarra et al. (2005) verified that hysteresis peak-oriented deterioration model is able to predict the inelastic dynamic response of a reinforced concrete structure during collapse more accurately. The proposed deterioration model has been used previously by many researchers (e.g.: Ibarra and Krawinkler, 2005; Lignos and Krawinkler, 2012).

5.2. SDOF model parameters

In this section, the mean values of ESDOF input parameters for each subclass corresponding to the Ibarra peak-oriented hysteresis model used in OpenSees platform are presented. Results of bilinear idealization of all subclasses are summarized in the form of the mean and standard deviation of T, η, and μ for each subclass. The

statistical values corresponding to the SDOF parameters of subclasses are listed in Table 1. Here, α_s represents the ratio of post yield to elastic stiffness, α_c is the ratio of the post-capping stiffness to the elastic stiffness, λ is the ratio of residual strength to the yielding strength, and γ is the hysteretic energy dissipation parameter.

Table 1. Proposed SDOF parameters for all building subclasses

Frame ID	T (sec)		η		μ		α_s (%)	α_c (%)	λ	γ
	Mean	Standard deviation	Mean	Standard deviation	Mean	Standard deviation				
RF1A	0.38	0.18	0.40	0.08	9.00	3.12	4	-20	0.20	800
RF1B			0.30	0.11	7.30	2.02	4	-25	0.20	400
RF1C			0.23	0.06	4.90	1.47	4	-30	0.20	200
RF2A	0.70	0.27	0.34	0.11	7.10	2.25	4	-20	0.20	800
RF2B			0.26	0.09	6.10	1.75	4	-25	0.20	400
RF2C			0.17	0.06	5.10	1.38	4	-30	0.20	200
RW1A	0.05	0.02	1.95	0.55	3.00	1.10	8	-20	0.20	1200
RW2A	0.15	0.05	1.30	0.36	2.70	0.90	8	-20	0.20	1200
RH1A	0.08	0.04	0.93	0.31	5.40	1.70	4	-20	0.20	1000
RH1B			0.77	0.25	4.50	1.40	4	-25	0.20	500
RH2A	0.43	0.18	0.59	0.17	4.90	1.40	4	-20	0.20	1000
RH2B			0.47	0.13	4.00	1.20	4	-25	0.20	500
MU1A	0.06	0.02	0.86	0.17	3.53	0.71	0	-20	0.20	600
MU1B			0.64	0.13	3.43	0.69	0	-25	0.20	300
MU1C			0.38	0.08	3.32	0.66	0	-30	0.20	150
MU2A	0.12	0.03	0.69	0.17	2.75	0.69	0	-20	0.20	600
MU2B			0.43	0.11	2.62	0.66	0	-25	0.20	300
MU2C			0.23	0.06	2.56	0.64	0	-30	0.20	150
MU3A	0.17	0.05	0.43	0.13	2.20	0.66	0	-20	0.20	600
MU3B			0.27	0.08	2.12	0.64	0	-25	0.20	300
MU3C			0.14	0.04	2.05	0.62	0	-30	0.20	150

6. GENERATION OF FRAGILITY CURVES

Fragility curve for a certain class of structural system is a continuous function describing the probability of exceeding a predefined damage level for specific levels of ground motion intensity. In this study, three structural performance levels are considered: Immediate Occupancy (LS_1), Life Safety (LS_2) and Collapse Prevention (LS_3).

6.1. Methodology

Figure (3) shows the schematic representation of the applied procedure for generation of fragility curve. In Figure 3-a, distribution of a sample response statistics is plotted. In this figure, the horizontal axis shows the ground motion intensity and the vertical axis presents the response parameter. The horizontal line labeled as LS_i represents the target limit state. The scattered data of the j^{th} ground motion intensity level (GMI_j) is selected in Figure 3-b. The conditional probability of attainment or exceedance of the i^{th} limit state (LS_i) at the j^{th} ground motion intensity level is calculated by using the following formula:

$$P\ D \geq LS_i | GMI_j] = \frac{n_A}{n_T} \quad (1)$$

where, n_A is the sum of responses equal or above the i[th] limit state, and n_T stands for the total number of responses at the j[th] ground motion intensity level. After repeating these processes for different intensity levels, the discrete fragility information presented in Figure 3-c can be obtained for a certain limit state. A cumulative lognormal distribution function is fitted on the obtained data with least squares technique as illustrated in Figure 3-d. To derive fragility curves for all subclasses, this process is repeated for three limit states and all 21 subclasses.

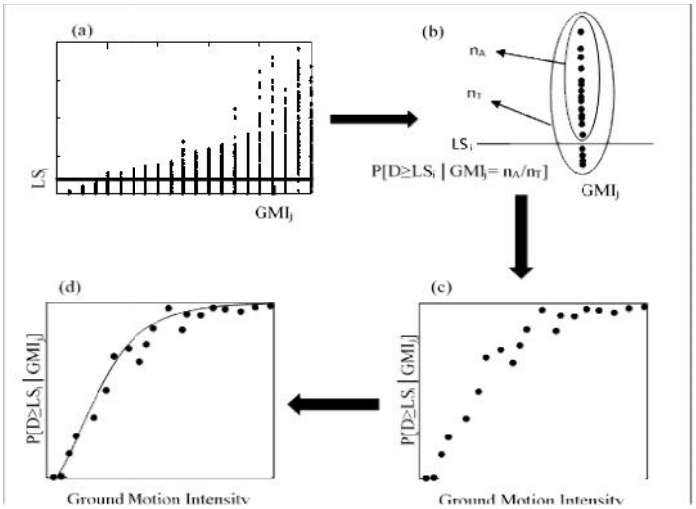

Figure 3. Schematic representation of the fragility curve generation procedure

6.2. Ground motion variability

Damage patterns monitored in the past events revealed that PGV and PGA correlate well with inelastic response of flexible structures (RC frame) and stiffer structures (masonry), respectively, (Erberik, 2008a; 2008b). Since the governing structural types in Erzincan include both reinforced concrete and masonry buildings, to provide a strong correlation between hazard parameters and nonlinear responses of the existing building stock, earthquake ground motions are separated into two groups: The first group is categorized according to PGV (for RC buildings) and the second group is classified with respect to PGA (for Masonry buildings) as intensity parameter. Overall, the selected synthetic records cover a broad range of magnitudes between 5 and 7.5. The closest distance to the fault plane varies between 0.26-17.55 km. In order to have an even distribution for responses of the structures, each ground motion set, which is categorized according to PGV or PGA, is subdivided into 20 intensity levels by considering intervals of PGV=5 cm/sec or PGA=0.05g, respectively.
In this study, to account for the variability in demand, for each ground motion set a total of 200 records are selected such that for each intensity level there are 10 time histories with different soil conditions, distance and magnitude values.

6.3. Structural simulations and response statistics

In this study, $T, \eta, and\ \mu$ parameters are considered as random variables. Lognormal distribution is assumed as the probability distribution function of the random variables since it results in positive values. Using Latin Hypercube Sampling method, for each of the random variables corresponding to the mean values of period, strength ratio, and ductility factor, 20 samples are generated. As a result, the sample size in each subclass is considered to be 20.The remaining model parameters including α_s, α_c, λ, and γ are assumed to be constant for all 20 simulated buildings from each subclass.
For a single subclass, since there exist 20 buildings, and the number of records in a specified intensity level (PGV or PGA) is 10, the number of response data points for an intensity level counts as 200. Since there are

totally 20 intensity groups, the number of SDOF analyses required to obtain the response statistics becomes 4000. NTHA is performed to reach the structural responses, which is assumed to be maximum ESDOF displacement.

6.4. Attainment of limit states

Attainment of limit states, which are defined as the capacity of structures at some predetermined thresholds is a significant part of fragility analysis. Previous studies demonstrate that limit states affect the resulting fragility curves considerably (Erberik 2008b). Therefore, they should be established with special care. In this study, instead of complicated approaches based on detailed behavior of members, constant (deterministic) values are assigned to limit states. Limit state values are selected according to the ones established by Erberik (2008a) and (2008b) for RC and masonry structural types in Turkey.

6.5. Results

Figures 4-5 show the final smooth fragility curves. Comparison of the results show that for a given ground motion level, as the number of stories increases, the potential of damage increases for all building types. Also, in all cases, as the level of compliance with seismic design and construction codes gets worse, the probability of exceeding the ultimate limit state (LS_3) increases. For immediate occupancy limit state (LS_1), regardless of the level of compliance of structures with seismic design codes, the results of subclasses with the same number of stories and structural system are close to each other. However, for life safety (LS_2) and especially for collapse prevention limit states, the results deviate from each other.

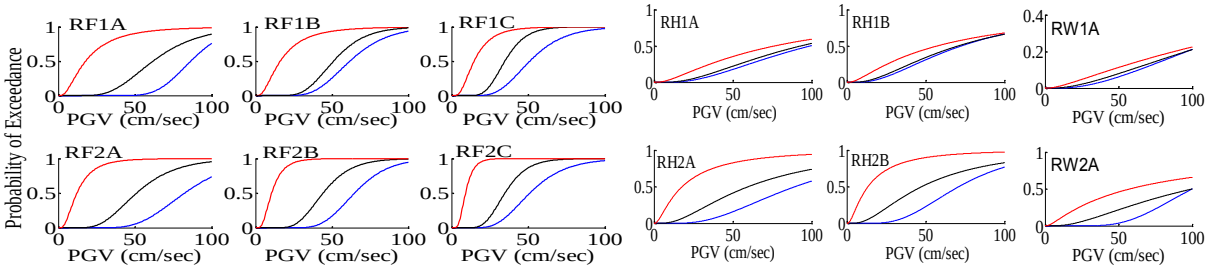

Figure 4. Fragility curves for RC subclasses using the first group of records categorized based on PGV where the red lines correspond to LS_1, the black lines to LS_2, and the blues line to LS_3

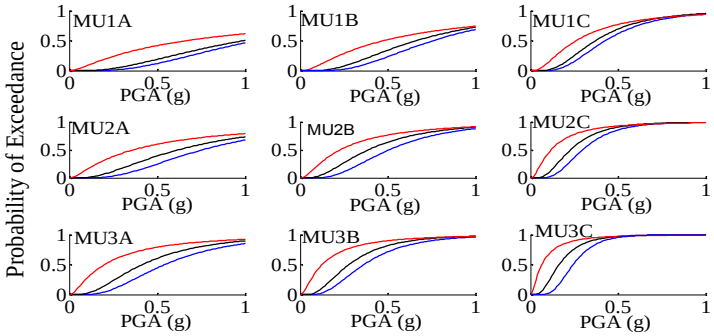

Figure 5. Fragility curves for masonry subclasses using the second group of records categorized based on PGA where the red lines correspond to LS_1, the black lines to LS_2, and the blue lines to LS_3

7. ESTIMATION OF DAMAGE

In this section, first the methodology is presented followed by a verification exercise where the estimated

damage for the 1992 Erzincan earthquake is compared with the observed one. Finally, the potential seismic damage for a scenario event of Mw=7 is presented as a prediction exercise.

7.1. Methodology

In the present study, among various damage parameters in the literature, (Lang et al. 2008, Bal et al. 2010), mean damage ratio (MDR) that expresses the disaggregated damage estimates with a single value as implemented by Askan and Yücemen (2010) is chosen. For the computation of MDR, damage probability matrix (DPM) as introduced by Whitman (1973) is employed. Each element of this matrix, denoted as P(DS, I), indicates the probability of experiencing a certain damage state (DS) when the structure under consideration is subjected to a specified ground motion with intensity level of I:

$$P_k\ DS, I\ = \frac{N(DS,I)}{N(I)} \tag{2}$$

where, N(I) is the number of k^{th}-type of buildings in the area subjected to a ground motion of intensity I and N(DS, I) is the number of structures in damage state (DS), among the N(I) buildings.
To express the damage ratios in a more comparable manner, the discrete values corresponding to each intensity level are converted to a single value as MDR. MDR is expressed in Equation (3) where, CDR(DS) represents the central damage ratio corresponding to damage state DS and it is defined as the ratio of the cost of repairing the earthquake damage to the replacement cost of the building.

$$MDR\ I\ = \sum_{DS} P_k\ DS, I\ .CDR(DS) \tag{3}$$

7.2. Applications in the study region

To evaluate the success of the proposed methodology in predicting actual damage distribution of the study area, the considered analysis is first applied for the 1992 Erzincan earthquake. Then, as a sample for prediction of potential losses, the seismic damage for scenario event of Mw=7 is hypothetically calculated. For this purpose, a total of 16 residential districts in Erzincan city with available building data are selected. The steps for damage assessment are summarized as follows:

1) For the simulation of the 1992 Erzincan earthquake (Mw=6.6) and scenario event with Mw=7, synthetic records for the selected residential areas are collected.
2) Since fragility curves of RC and masonry buildings are derived in terms of PGV and PGA, respectively; PGA and PGV values corresponding to centroid of each considered district are obtained from the synthetic records.
3) For the selected districts, percent distribution of the buildings with respect to the structural type as well as number of stories is attained.
4) Using the derived fragility curves, MDR for all building types in each district under the given ground motion value are obtained.
5) Finally, through percent distribution of buildings in the selected locations, a single MDR is calculated for each residential area.

Results of MDR for the selected residential districts are listed in Table 2. It is worth to mention that the observed MDR values for the 1992 Erzincan earthquake are adopted from Sucuoğlu and Tokyay (1992), Şengezer (1993), and Erdik et al. (1994). Comparison of the observed and estimated damage levels for the 1992 Erzincan earthquake demonstrates that for almost 75% of the residential areas the results are in close agreement.For the other locations, the estimated damage levels are found to be larger than the observed ones, which indicates that the proposed methodology yields conservative conclusions. After validating the method for the 1992 earthquake, the anticipated potential sesmic damage for the secenario event of Mw=7 is also computed and presented in

Table 2. The damage estimates for the scenario event of Mw=7 reveal that six of the residential areas experience severe damage (50%<=MDR<=90%). However, the estimated damage in the rest of the residential areas are moderate (10%<=MDR<=50%).Therefore, for scenario event of Mw=7, the estimated damage levels show that the Erzincan city center is subjected to the moderate to heavy damage levels (10%-90%) in the selected residential areas which is consistent with the regional seismicity and the structural vulnerability.

Table 2. Observed and estimated MDR for the 1992 Erzincan earthquake and the scenario earthquake of Mw=7

Street	Lat.	Long.	1992 Erzincan Earthquake		Scenario event with Mw=7.0
			Observed MDR(%)	Estimated MDR (%)	Estimated MDR(%)
İNÖNÜ	39.7505	39.4857	16.78	18.86	55.46
İZZETPAŞA	39.7401	39.5083	Not available	40.29	52.14
AKŞEMSETTİN	39.7506	39.5148	39.00	41.15	61.19
ARSLANLI	39.7595	39.4830	20.84	20.84	43.00
ATATÜRK	39.7492	39.4955	5.89	13.47	44.64
BAHÇELİEVLER	39.7512	39.4757	9.00	20.89	45.29
BARBAROS	39.7542	39.5037	15.00	34.22	46.00
CUMHURİYET	39.7594	39.4967	35.00	37.81	41.13
ERGENEKON	39.7516	39.4641	Not available	5.60	69.36
HALİTPAŞA	39.7440	39.4789	13.54	15.57	48.65
HOCABEY	39.7416	39.4849	13.83	17.79	37.28
KIZILAY	39.7448	39.4897	29.65	28.36	41.74
MİMAR SİNAN	39.7430	39.4662	Not available	28.66	28.17
YAVUZ SELİM	39.7581	39.4738	35.10	40.60	73.28
YENİ	39.7574	39.4901	Not available	20.74	48.50
FATİH	39.7461	39.5110	31.22	32.36	54.81

8. CONCLUSIONS

In this study, seismic damage estimation in Erzincan for the 1992 event and a scenario earthquake is performed using both regional seismicity and local building data. The match between the observations and computed results show the efficiency of considering the specific characteristics of the earthquake rupture through ground motion simulations as well as local building information in the predicted damage estimates. The estimated damage levels in the city center reveal that Erzincan is under significant seismic threat due to its close distance from the fault system in the North, soft soil conditions within Erzincan basin as well as the seismic vulnerability of the building stock in the region. Thus, before another major earthquake is experienced in the region, the existing buildings must be evaluated for seismic safety in detail to avoid potential future losses.

It must be noted that the results presented herein contain inherent uncertainties arising from various sources such as modeling errors involved with the ground motion simulation technique, selection of input parameters, building data, fragility and damage estimation methodologies. Another major source of error arises from subjectivity in assigning damage states for the buildings in the field. Therefore, although the results presented herein are attained from physical and realistic models, they should be evaluated carefully in the existence of the mentioned inherent model and data uncertainties.

REFERENCES

Askan, A. and Yucemen, M.S. (2010). Probabilistic methods for the estimation of potential seismic damage: Application to reinforced concrete buildings in Turkey. *Structural Safety* ***32*****:4**, 262-271.

Askan, A., Sisman, F.N. and Ugurhan, B. (2013). Stochastic strong ground motion simulations in sparsely monitored regions: A validation and sensitivity study on the 13 March 1992 Erzincan (Turkey) earthquake. *Soil Dynamics and Earthquake Engineering* **55**, 170-181.

Bal, I.E., Bommer, J.J., Stafford, P.J., Crowley, H. and Pinho, R. (2010). The influence of geographical resolution of urban exposure data in an earthquake loss model for Istanbul. *Earthquake Spectra* **26**, 619–634.

Boore, D.M. (1983). Stochastic simulation of high-frequency ground motions based on seismological models of the radiated spectra. *Bulletin of Seismological Society of America* **73**, 1865–1894.

Erberik, M.A. (2008,a). Generation of fragility curves for Turkish masonry buildings considering in-plane failure modes. *Earthquake Engineering & Structural Dynamics* **37:3**, 387-405.

Erberik, M.A. (2008,b). Fragility-based assessment of typical mid-rise and low-rise RC buildings in Turkey. *Engineering Structures* **30:5**, 1360-1374.

Erdik, M., Yüzügüllü, O., Karakoc, Yilmaz, C.and Akkas, N. (1994). March 13, 1992 Erzincan (Turkey) earthquake, Earthquake Engineering, Tenth World Conference, Balkema, Rotterdam.

Ibarra L.F. and Krawinkler, H. (2005). Global collapse of frame structures under seismic excitations. Rep. No. TB 152, The John A. Blume Earthquake Engineering Center, Stanford University, Stanford, CA.

Ibarra, L.F., Medina, R.A. and Krawinkler, H. (2005). Hysteretic models that incorporate strength and stiffness deterioration. *Earthquake Engineering and Structural Dynamics* **34**, 1489–1511.

Lignos, D.G. and Krawinkler, H. (2012). Development and Utilization of Structural Component Databases for Performance-Based Earthquake Engineering. *Journal of Structural Engineering, ASCE* **139:8**, 1382-1394.

Mai, P.M., Imperatori, W. and Olsen, K.B. (2010). Hybrid broadband ground-motion simulations: Combining long-period deterministic synthetics with high-frequency multiple S-to-S back-scattering. *Bulletin of Seismological Society of America* **100:5A**, 2124-2142.

Motazedian, D. and Atkinson G.M. (2005). Stochastic finite-fault modeling based on a dynamic corner frequency. *Bulletin of Seismological Society of America* **95**, 995–1010.

Olsen, K.B., Archuleta, R.J. and Matarese, J.R. (1996). Three-dimensional simulation of a magnitude 7.75 earthquake on the San Andreas fault.*Science* **270**, 1628-1632.

OpenSees 2.4.5. Computer Software, University of California, Berkeley, CA. Retrieved from http://opensees.berkeley.edu

Park, Y.J., Reinhorn, A.M. and Kunnath, S. K. (1987). IDARC: Inelastic Damage Analysis of Reinforced Concrete Frame –Shear all Structures, Technical Report NCEER-87-0008, State University of New York at Buffalo.

Lang, D.H., Molina, S. and Lindholm, C.D. (2008). Towards near-real-time damage estimation using a CSM-based tool for seismic risk assessment. *Journal of Earthquake Engineering* **12: 2**, 199–210.

Sucuoğlu H. and Tokyay M. (1992). 13 Mart 1992 Erzincan earthquake engineering report, civil engineering department, Ankara, pp: 102.

Sucuoğlu, H. and Erberik, M.A. (2004). Energy Based Hysteresis and Damage Models for Deteriorating Systems. *Earthquake Engineering and Structural Dynamics* **33**, 69-88.

Sørensen, M.B. and Lang, D.H. (2014). Incorporating Simulated Ground Motion in Seismic Risk Assessment-Application to the Lower Indian Himalayas. *Earthquake Spectra* **31:1**, 71-95.

Şengezer, B.S. (1993). The Damage Distribution during March 13, 1992 Erzincan Earthquake, proceedings, 2nd National Earthquake Engineering Conference, pp: 404-415.

Ugurhan, B. and Askan, A. (2010). Stochastic strong ground motion simulation of the 12 November 1999 Düzce (Turkey) earthquake using a dynamic corner frequency approach. *Bulletin of Seismological Society of America* **100**, 1498-1512.

Ugurhan, B., Askan, A. and Erberik, M.A. (2011). A methodology for seismic loss estimation in urban regions based on ground-motion simulations. *Bulletin of the Seismological Society ofAmerica* **101**, 710–725.

Whitman, R.V., Anagnos, T., Kircher, C.A., Lagorio, H.J., Lawson, R.S. and Schneider, P. (1997). Development of a national earthquake loss estimation methodology. *Earthquake Spectra* **13**, 643–661.